Experimental Study on the Spalling behaviour of Ultra-High Strength Concrete in Fire

Yong Du [a*, c], Hong-Hui Qi [a, c], Shan-Shan Huang [b], J.Y. Richard Liew [c]

[a] *College of Civil Engineering, Nanjing Tech University, Nanjing, 211816, China*

[b] *Department of Civil and Structural Engineering, The University of Sheffield, Sheffield, S1 3JD, UK*

[c] *Department of Civil and Environmental Engineering, National University of Singapore, Singapore, 119077, Singapore*

ABSTRACT

High strength construction materials are now attractive owing to their economic and architectural advantages. The higher the material strength, the smaller member size is required. Ultra-high strength concrete (UHSC) encased columns are being developed for the erection of high-rise buildings due to their higher load bearing capacity and smaller cross section size compared to normal strength concrete encased columns. When the UHSC is subject to elevated temperature, explosive fire-induced spalling is more often observed than in normal strength concrete. The consequence of spalling could cause serious life loss and damage to the close key infrastructure. Spalling is mostly due to the UHSC increased density, lower permeability and brittleness. Most of the previous studies show that polypropylene fibres have been found effective in preventing fire spalling. The aim of this experimental study is to discover the minimum polypropylene fibre dosage to control the fire spalling of steel fibre reinforced concrete of 115-135 MPa strength. The experimental study was carried out on 15 concrete specimens with different parameters and two fibre-reinforced concrete encased columns exposed to ISO 834 fire. The study indicates that a polypropylene fibre dosage of 1.365 kg/m^3 can prevent the 115-135 MPa ultra-high strength concrete from explosive fire spalling. This polypropylene fibre dosage is lower than that proposed in Eurocode 2, which is 2 kg/m^3. The proposed lower polypropylene fibre dosage can potentially bring sustainability (use less polypropylene fibres that are made of crude oil) and economy, as well as improve constructability by improving the workability of fresh concrete. It is also found steel fibres may relieve the fire spalling but

* Corresponding author.

E-mail address: yongdu_mail@njtech.edu.cn (Yong Du)

not adequate to prevent spalling. Moreover, there is no significant effect of the size and inner temperature of the centre of the concrete specimen on spalling.

Keywords: Ultra-High Strength Concrete; Fire; Polypropylene Fibre; Fire Spalling; Steel Fibre Reinforced Concrete.

1. Introduction

In recent years, Ultra-High Strength Concrete (UHSC) can be manufactured by more and more concrete plants due to the increasing availabilities of a variety of additives such as silica fume [1-4] and water reducing admixture [5-7]. The wider availability of UHSC has triggered the developed UHSC encased steel composite columns for high-rise buildings, due to their higher load bearing capacity and smaller cross section size compared to normal strength concrete encased columns [8-11]. Fig. 1 displays the practical case and typical cross section of concrete encased columns. However, UHSC exhibits more brittle behaviour comparing with normal strength concrete (NSC), which results in low resistance to crack propagation. Numerous tests [12-14] have found that the use of steel fibres could significantly improve the ductility of concrete and prevent cracking at ambient temperature. Therefore, steel fibre reinforced UHSC is proposed for the concrete encased steel composite columns in this study.

When concrete is exposed to elevated temperatures, physical and chemical changes, such as vaporization of water and C-S-H dehydration have been observed [15-17], which then reduce the durability and strength of concrete. Concrete also experiences explosive fire-induced spalling when exposed to rapid heating, like a fire [18-25]. Explosive fire-induced spalling is defined as the violent expulsion of shards from the hot surface of concrete as the temperature increases rapidly, which may cause more casualties and damage to the surrounding environment. Recent tests [26, 27] have shown that the post-fire residual compressive strength and post-fire residual aggregate-mortar bonding strength of high strength concrete are higher than those of NSC if explosive spalling does not occur. Besides, the fire spalling risk increases as the concrete strength increases, and so UHSC is particularly vulnerable to fire spalling. It is most owing to increased density, lower permeability and brittleness in fire conditions [22-24]. Low water-cement (w/c) ratio and silica fume, which are essential for UHSC, lead to lower permeability of UHSC compared with NSC. Kalifa et al. [22] indicated that as a consequence of lower permeability, higher pore pressure, leading to fire spalling, is attributed to the large difference in the thermodynamic conditions reached in the concrete. Experimental studies [24] have shown that the explosive spalling of high strength concrete is affected by various factors, including heating rate, type of aggregate, dimension of samples, reinforcement arrangement, moisture content and concrete density.

There are two most mentioned theories on the mechanism of fire spalling [21, 22, 25, 28, 29]. One is related to the thermo-mechanical process (thermal stresses theory), which induces spalling owing to the high thermal stress between the heated surface and the moisture clog, where the pores are saturated by condensed vapour. A steep thermal gradient develops since the temperature at the moisture clog is close to 100 °C and the surface temperature increases rapidly, which induces high thermal stresses. The other one is related to the thermo-hydral process (pore pressure theory), which is associated with the vaporization and pores. The high rate of vaporization in the moisture clog, as well as the thermal dilation of vapour and air due to heating, induces higher pore pressure. Concrete spalling would finally occur if the pore pressure exceeds the tensile strength of the concrete. However, Li at al. [23] measured the pore pressure of ultra-high-performance concrete with silica fume. It was found that the maximum pore pressure is much lower than the tensile strength of the concrete, indicating that tensile strength may not be an adequate reasonable failure criterion for explosive spalling. One possible reason was put forward that spalling is generated by a step pressure difference, causing the collapse of the concrete matrix between the pores. Heo et al. [25] drew a conclusion that the spalling mechanism of high strength concrete could be explained using either the thermal stresses theory, pore pressure theory or a combination of both. Besides, Liu et al. [30] presented a new perspective that there were three types of fire-induced concrete spalling depending on the mechanisms, comprising thermo-hygral, thermo-mechanical and thermo-chemical spalling. However, there is neither full agreement on the spalling mechanism, nor fully accepted predictive modelling of explosive fire spalling.

Adding polypropylene (PP) fibres to UHSC mixes is the most accepted method to improve their permeability at high temperature and to reduce the fire spalling risk. The dense pore structure of UHSC would make the flow of vapour more difficult than that of NSC and accelerate the pore pressure rise in fire. PP fibre's melting point is low, which is 170 ℃ in general. At high temperature, the PP fibres would melt, so that the vapour can evacuate through the connected porous network [25, 31]. Suhaendi et al. [32, 33] reported that fibres of longer lengths are more efficient in fire spalling control than those of shorter lengths, due to the effect that long fibres are beneficial to bridge the isolated pores. However, conflicting result was shown in other studies [34, 35]. Based on tests on small size specimens, Heo et al. [25]

proposed a model for calculating the optimum fibre length, but further research is needed on the effect of specimen size. The Eurocode 2 [36] recommends that more than 2 kg/m^3 (0.22% by volume) of polypropylene fibres should be added to the concrete of grades C80/95 to C90/105. Xiong et al. [37] investigated UHSC with different PP fibre dosages in fire. The test results indicated that 0.91 kg/m^3 PP fibres is effective in preventing the fire spalling of UHSC of strength over 150 MPa heated to 800 °C at different heating rates (5 °C/min and 30 °C/min). However, the optimum dosage of PP fibre for UHSC of 115-135 MPa has not been well studied.

The effect of steel fibres on the fire spalling of concrete is also under discussion. Kodur et al. [24, 38] carried out fire resistance experiments on five types of reinforced concrete columns, and the results showed that the use of steel fibres could reduce fire spalling and improve the fire resistance of high strength concrete columns. However, Bei et al. [39, 40] reached a different conclusion, which is that steel fibre can only delay the fire spalling time of UHSC under rapid heating, but not prevent fire spalling. It may be attributed to the significantly degraded bond strength between the steel fibre and concrete matrix with increasing temperature, according to Abdallah [41]. The combined use of PP and steel fibres was also investigated [23, 42], and Li [23] demonstrated that the PP and steel fibre blends could prevent explosive spalling as the strain incompatibility between the steel fibres and concrete matrix enhances the connectivity of the PP fibre tunnels.

Although many researchers [23, 37, 52] have focused on the PP fibre dosage against explosive spalling, it is critical that the spalling test results could vary depending on other effective parameters. Appendix A shows the spalling test results in previous studies considering the effect of specimen dimension, 28-day compressive strength, aggregate type, w/b and fibre dosages. It could be found that PP fibres show the significant effect on reducing the explosive spalling. The w/b of UHSCs is in a range of 0.11 ~ 0.22, which is so low that the risk of spalling significantly increases as comparing with NSC. There is no control group in Appendix A, which shows so many factors can affect the risk of UHSC spalling. Against such background, the present study focused on the UHSC with basalt aggregate in the range of cubic strength from 115 MPa to 135 MPa. The test results can provide additional information on the UHSC spalling.

This study aims to study the fire spalling behaviour of steel fibre reinforced UHSC with PP fibres of a cubic strength of 115-135 MPa and to determine the optimum PP fibre dosage to prevent explosive fire spalling. The paper focuses on the fire spalling test of UHSC. The effect of steel fibre on spalling resistance has also been investigated. In addition, two UHSC encased columns were tested at high temperature to validate the reliability of the proposed dosage of PP fibres for fire spalling control on structural member level. The fresh properties and porosity of UHSC with different w/b and fibre contents were also measured.

2. Experiments on UHSC

2.1 Materials and mix design

The UHSC mix consists of P·Ⅱ Type 52.5 Onoda cement, river sand, 5-15 mm basalt aggregate, superplasticizer, polypropylene fibres and steel fibres. The PP and steel fibres are shown in **Fig. 2** and their properties are listed in **Table 1**. The main ingredient of the superplasticizer is polycarboxylic acid.

Two UHSC mixes were adopted, as listed in **Table 2**. Two water/binder (w/b) ratios, 0.15 and 0.18, were adopted. The specimens were cast and stored for 24 hours in the laboratory environment before demoulding. They were then demoulded, labelled and cured in 98% relative humidity at 20 °C for 27 days. The 28-day cube compressive strength of concrete were measured from 100×100×100 mm cubes. The strengths of the plain UHSC mixes were tested and listed in **Table 2**. For each case, three tests were repeated. The average values are 117 MPa for Mix I (w/b = 0.18) and 134 MPa for Mix II (w/b = 0.15).

2.2 Fresh properties

The key aim of the fresh property tests was to evaluate the workability of the UHSC **[43]**. The fresh concrete properties were tested according to relevant standards for self-compacting concrete **[43-45]**. The slump-flow and T_{500} time were measured by slump-flow tests to assess the concrete's flowability and its flow rate in the absence of obstructions, as shown in **Fig. 3(a)**. J-ring tests were conducted to investigate the flowability and passing ability of concrete, as presented in **Fig. 3(b)**. L-box tests were carried out to assess the passing ability of concrete, flowing through tight openings including spaces between reinforcing bars and other obstructions without segregation or blocking, as shown in **Fig. 3(c)**.

In the slump-flow tests, the largest diameter of the flow spread and the diameter at the perpendicular direction were measured. The mean value of these two measurements was recorded as S in **Table 3** to the nearest 10 mm. it is found that the higher the value of S is, the larger the concrete ability is to fill the formwork. T_{500} is the recorded time (to the accuracy of 1 s) when the flow spread reaches 500 mm. A lower T_{500} indicates a greater fluidity or smaller workability loss. Similar to the slump-flow tests, in the

J-ring tests, the largest diameter of the flow spread, and the diameter at the perpendicular direction were measured. Their average was recorded as S_J in **Table 3** to the nearest 1 mm. The passing ability PA in **Table 3** is given by:

$$PA = S - S_J \tag{1}$$

In the L-box tests, when the concrete movement ceased, the depth of concrete left behind the gate was measured as H_1, and the depth of concrete passed through the gate was measured as H_2. The passing ability is represented as H_2/H_1. A lower PA or higher H_2/H_1 value indicates a better passing ability. Haddadou et al. **[43]** suggest that H_2/H_1 ranging from 0.8-1.0 is acceptable for self-compacting concrete.

Table 3 shows the fresh properties of UHSC. To sum up, the slump flow diameter of all concretes were in the range of 450-750 mm; the slump flow time was in the range of 5-14 s; the PA values of the J-ring tests were in the range of 20-70 mm and the H_2/H_1 ratios of the L-box tests was in the range of 0-0.92. Plain UHSC of w/b = 0.18 shows a greater filling ability than that of w/b = 0.15 due to higher S. This indicates that the w/b ratio is critical for the flowability of UHSC. The addition of fibres can significantly decrease the filling and passing abilities of UHSC. Comparing the results of Samples 1-4 in **Table 3**, it can be found that the flowability decreases with an increase in steel fibre dosage. The effect of PP fibres on flowability is similar to that of steel fibres, by comparing Samples 5, 9, 10 and 11. The S value of Sample 6 with steel fibre dosage of 39.25 kg/m^3 (0.5% by volume) was 620 mm; this value dropped to 510 mm for Sample 11 with PP fibre dosage of 2 kg/m^3 (0.22% by volume). The H_2/H_1 ratio of Sample 6 is 0.85; this ratio dropped to 0.25 for Sample 11. This implies that PP fibres have more impact on the flowability compared to steel fibres of the same dosage (by volume). In addition, Sample 13 was difficult to mix; its S value was 450 mm and so T_{500} could not be measured; its PA value was 70 mm and the H_2/H_1 ratio was 0, confirming the very low flowability of the mix, which might result from the excessive dosage of fibres. For constructionability, this paper recommends not to add more than 78.5 kg/m^3 steel fibres (1% by volume) and more than 2 kg/m^3 PP fibres (0.22% by volume) to UHSC at the same time.

2.3 Porosity

Mercury intrusion porosimetry tests were carried out to measure the porosity, which might affect the occurrence of fire spalling **[39, 46, 52, 57]**. The MIP tests were performed on 10×10×10 mm cubes using Poremaster GT-60 to measure the porosity of plain UHSC with different w/b. The MIP test specimens were cut from bigger UHSC specimens of different w/b.

Fig. 4 shows the MIP results of plain UHSC with two w/b ratios at ambient temperature. The cumulative intrusion volumes of these two UHSC mixes follow the same increasing trend, as shown in Fig. 4, indicating that the microstructures of the two mixes are similar. The porosity of each UHSC was calculated automatically by Poremaster GT-60. The porosity of the UHSC mix of w/b = 0.18 is 4.25%, and that of the UHSC mix of w/b = 0.15 is 2.34%, implying that the mix of lower w/b ratio might have a denser microstructure compared to the mix of high w/b ratio. The effect of porosity on the fire spalling behaviour is discussed in Section 2.5.4.

2.4 Fire spalling tests

In this paper, PP fibre dosages of 0 kg/m^3, 0.91 kg/m^3, 1.183 kg/m^3, 1.365 kg/m^3, 2 kg/m^3, 2.73 kg/m^3 and 4.55 kg/m^3 were used, and the dosages of steel fibre adopted were 0 kg/m^3, 11.775 kg/m^3, 23.55 kg/m^3 and 78.5 kg/m^3 in the fire spalling tests. Two specimen sizes, Ø300×300 mm cylinders and Ø100×200 mm cylinders, were adopted to study the specimen size effect. Table 4 summarizes the details of the UHSC specimens of the fire spalling tests.

The spalling tests began on the 28th day after casting. All tests were completed within 3 days. Fire spalling tests on 15 UHSC specimens were conducted using a gas furnace. The heat apparatus was a split-tube furnace with a three-zone (top, middle and bottom) configuration and a side view window. A type K thermocouple was mounted at the centre of each zone to ensure the temperature distribution within the furnace is uniform. Fig. 5 shows the internal dimension of the furnace. The furnace could heat up to 1250 °C following ISO834 fire. The specimens were heated in the gas furnace one by one. In order to protect the furnace from the explosive spalling of concrete, a steel cage as shown in Fig. 6 was employed. A thermocouple was embedded in the centre of each specimen to measure its inner temperature. After each fire test, the cylinder sample was wrapped by a piece of graph paper to copy the spalling profile via pencil rubbing.

Many researchers have investigated the effect of heating regime on fire spalling. Fellcetti [47] studied the spalling damage of UHSC heated at a slow rate of 1 °C/min. Li [23] tested fibre-reinforced UHSC at the rate of 2 °C/min, and Durrani [48] explored the spalling behaviour of high strength concrete heated rapidly at 30-90 °C/min. Bei et al. [39] suddenly put the UHSC specimen into the preheated furnace with

1000 °C. However, the increase rate of temperature as mentioned above cannot follow the ISO834 standard fire in which most of members always experience as fire test operated.

Thus, the ISO 834 [49] standard fire curve was employed in the fire spalling tests of this research for standardisation. Fig. 7 shows the comparison between the temperature-time relationship of ISO 834 and that measured in the furnace without specimens. The good agreement of them indicates that the furnace could simulate the heating rate of ISO 834.

In addition to the heating regime, the loading is also a critical factor to affect the fire spalling. A general opinion is that the probability and severity of spalling increase with compressive loading increasing. Boström et al. [50] studied the effect of loading level on the fire spalling by pre-loading a compressive force on the specimens in fire. The results showed that the probability as well as the severity of spalling is much greater than that of specimens without load. Hence he suggested that the compressive load should be taken into account during the concrete spalling test. Compared to most tests on concrete specimens without loading, although Ali [51] reported that the increase of loading level did not improve the possibility of concrete spalling, most previous tests on columns considered the effect of the loads on explosive spalling [51-54].

In this paper, all cylinder specimens heated without loading investigated the effect of fibre dosage and size on UHSC spalling, and then, the fire tests of full scale UHSC encased columns were carried out to explore the effect of loading on UHSC spalling.

2.5 Test results and discussions

Table 5 shows the results of the spalling tests. The 28-day cube compressive strengths of the specimens are also listed, which are between 115 MPa and 135 MPa, all falling into the targeted range.

2.5.1 Failure modes

The failure modes of the specimens are shown in Figs. 8, 9 and 10. Due to the fully enclosed furnace, the colour change of the specimens during the heating time could not be observed. Most specimens showed the similar colour of greyish white after exposed to elevated temperatures, except the collapsed.

In order to describe the magnitude of fire spalling, visual evaluation classified specimens as having ‘slight damage’, ‘moderate damage’, ‘great damage’, ‘intensive damage’ and ‘collapse’ after the tests [55]. The spalling depth d_s and spalling area ratio δ_s, were obtained. The maximum spalling depth was measured as the vertical distance from the heated surface before spalling to the deepest spalled surface. The spalling area ratio δ_s is the ratio between the spalled area A_s and the total heated surface area A:

$$\delta_S = \frac{A_S}{A} \tag{2}$$

Fig. 8 shows the failure modes of UHSC1 to UHSC5 with w/b of 0.18 and different fibre dosages. The UHSC specimen with 0.91 kg/m^3 PP fibres shows few cracks on the top of the specimen, classified as 'slight damage', as shown in **Fig. 8(a)**. It indicates that the 0.91 kg/m^3 (0.1% by volume) PP fibre dosage is likely to be close to the critical dosage which could control spalling. There is almost no damage in UHSC with PP fibres as shown in **Figs. 8(b), (c) and (d)**. Their spalling depths and spalling area ratios are all zero. Specimen UHSC5 without PP fibre spalled so intensively that it collapsed and only debris as shown in **Fig. 8(e)** was left. This spalling was very explosive and with very loud sounds.

The failure modes of the series of tests on the UHSC6 to UHSC12 with w/b ratio of 0.15 are shown in **Fig. 9**. There is almost no damage in UHSC6 with 2.73 kg/m^3 PP fibres and 11.775 kg/m^3 steel fibres, UHSC7 with 4.55 kg/m^3 PP fibres and 11.775 kg/m^3 steel fibres and UHSC8 with 2 kg/m^3 PP fibres and no steel fibre as shown in **Figs. 9(a), (b) and (c)**, respectively. Their spalling depths and spalling area ratios are all zero. **Fig. 9(d)** shows the intensive damage in UHSC9 with no PP fibre and 78.5 kg/m^3 steel fibres. Its spalling depth is 47 mm, and the spalling area ratio is 63%. This indicates that the PP fibre is the main contributor of spalling mitigation, not the steel fibre. **Figs. 9(e), (f) and (g)** show the failure modes of UHSC with PP fibre dosage lower than 2 kg/m^3. The spalling depth of UHSC10 with 0.91 kg/m^3 PP fibres is 38 mm, and its spalling area ratio is 28%. The spalling depth of UHSC11 with 1.183 kg/m^3 PP fibres drops to 24 mm, and the spalling area ratio drops to 9%. This indicates that the effect of PP fibre on spalling mitigation depends on the dosage. There is almost no damage in UHSC12 with 1.365 kg/m^3 PP fibres as shown in **Fig. 9(g)**. This dosage is lower than that of 2 kg/m^3 recommended in EC2 **[36]**.

Fig. 10 shows the failure modes of UHSC13 to UHSC15 with w/b of 0.15 and smaller size to investigate the effect of size. Compared to UHSC10, the spalling depth of UHSC13 with the same fibre dosage drops to 13 mm, and its spalling area ratio is 28%. Similarly, compared to UHSC11, the spalling depth of UHSC14 with the same fibre dosage drops to 6 mm, but its spalling area ratio increases to 18%. There is almost no damage in UHSC15 with 1.365 kg/m^3 PP fibres as shown in **Fig. 10(c)**. It further proves that 1.365 kg/m^3 PP fibres is an adequate dosage to prevent spalling.

2.5.2 Temperature analysis

Fig. 11 shows the development of temperatures over time at the centres (centroid of the cross section at mid height) of typical specimens. The specimens of relatively lower PP fibre dosage (up to 1.365 kg/m^3) were tested first. The test durations were initially set as 120 minutes. None of those specimens spalled. It was expected that the remaining specimens (of PP fibre dosage >1.365 kg/m^3) would bear even less spalling risk. Therefore, the durations of the following tests were shortened to 60 minutes. On a separate note, explosive spalling occurs within 30 mins of heating in most cases. Therefore, either 60 mins or 120 mins of heating are adequate and should not affect the comparability of the test results.

After around 50 minutes of heating, the temperature at the centre of UHSC5 suddenly rose to close to the furnace temperature, due to the exposure of thermal couple when explosive spalling occurred. Except UHSC5, the heating rates within the other specimens illustrated in **Fig.11** are similar to each other. However, there was almost no spalling in UHSC2, UHSC7 and UHSC12, whereas there was moderate spalling in UHSC10 and UHSC11. This indicates that there is no obvious relationship between the inner temperature of concrete and spalling.

2.5.3 The effects of specimen size

Two specimen sizes have been adopted for specimens of the same water binder ratio (0.15) and of the same set of fibre dosages, as shown in **Table 4**. Specimens UHSC10, UHSC11 and UHSC12 are of 300 mm diameter and 300 mm height; UHSC13, UHSC14 and UHSC15 are of 100 mm diameter and 200 mm height. Among UHSC10-15, all specimens of PP fibre dosage lower than 1.365 kg/m^3 experienced moderate spalling. However, the spalling magnitude of the smaller specimens seemed to be less than those of the bigger specimens, see **Figs. 9(e), (f)** vs. **Figs. 10(a), (b)**. The spalling depth of UHSC13 decreased down to 46.4% comparing with that of UHSC10 using the same fibre dosage, and the spalling area ratios of them were the same. Similarly, the spalling depth of UHSC14 reduced down to 25% comparing with that of UHSC11, and the spalling area ratio of UHSC14 was twice of that of UHSC11.

There is no crack on the outer surfaces of specimens with 1.365 kg/m^3 PP fibres after heating. For both specimen sizes, the PP fibre dosage of 1.365 kg/m^3 (0.15% by volume) was effective in mitigating the explosive spalling under the testing condition described previously.

2.5.4 The effects of porosity

Zegardło et al. [56] stated that the porous structure of ceramic aggregate may facilitate the water vapor's diffusion from cement paste into the interior of aggregate's grain, which reduces the likelihood of fire spalling occurrence. Rossino et al. [57] studied the heat-induced microstructural changes of high-performance concrete and confirmed that the total porosity plays an important role in moisture transport and vaporization. Mindeguia et al. [58] reported that the effect of PP fibre on reducing the fire spalling of NSC with 40 MPa was governed by the increase of permeability of the exposed concrete, that is both porosity and pore connectivity. In present study the porosity test rather than permeability test was measured due to limited performance of instrument. Further study should be carried out to explain the effect of pore connectivity on UHSC spalling.

As mentioned in Section 2.3, the representative porosity of the UHSC mix of w/b = 0.18 (UHSC1-5) is 4.25%, and that of the UHSC mix of w/b=0.15 (the rest of the specimens) is 2.34%. Fig. 12 shows the 28-day cubic compressive strength against porosity. Generally, the concrete with lower porosity has higher compressive strength. The porosity is greater than 10%, whereas the 28-day cubic compressive strength is smaller than 60 MPa. When the porosity of the high strength concrete (HSC) is smaller than 6%, the compressive strength of it tends to exceed 100 MPa. Thus, the UHSC specimens in this study also have the quite low porosity comparing with the HSC and NSC.

The range of porosities varied in this study is small given the nature of UHSC, likely explaining the little influence of porosity on fire spalling occurrence. In addition, it should be reasonable to assume that the moisture contents of the specimens of the same w/c ratio are similar given that the specimens are cured and stored in the same condition (in 98% relative humidity at 20 °C) according to EN 206-1:2000.

Figs. 8(e) and 9(d) show the spalling of UHSC with no PP fibre, respectively. This indicates that the porosities of UHSC covered by this study did not make a difference to the spalling under the testing conditions. Taking into account the low porosity of all UHSC, it could be concluded that the effect of porosity without considering pore connectivity is limited. However, explosive spalling is prevented due to the addition of PP fibres to both base mixes, producing the connected porous network after the melting and degradation of them. Previous studies [25, 31-35, 46, 57] support this opinion as well. Further study is needed to measure the post-heating porosity of UHSC with PP fibres.

2.5.5 The effects of PP fibres

It is clear from both this and previous research, PP fibre is effective in reducing the fire spalling risk. However, it is wasteful and costly, as well as reduces the workability of fresh concrete to use too much PP fibres. Therefore, this study also aims to determine the optimum dosage of PP fibre for 115-135 MPa concrete.

Figs. 8, 9 and 10 show the failure modes of UHSC specimens with PP fibre dosages ranging from 0.91 kg/m^3 to 4.55 kg/m^3. Moderate spalling was observed from the specimens of PP fibre dosages lower than 1.365 kg/m^3, as shown in **Figs. 8(a), 8(e), 9(d), 9(e), 9(f), 10(a) and 10(b)**. With PP fibre dosages equal to or larger than 1.365 kg/m^3, no spalling was observed. For the specimens tested under the testing condition described in this paper, 1.365 kg/m^3 seems to be the optimal PP fibre dosage for preventing fire spalling. Therefore, this paper recommends a PP fibre dosage of 1.365 kg/m^3 (0.15% by volume) as the optimum dosage to prevent the explosive fire spalling of UHSC, less than the dosage recommended in EC2 **[36]**.

Similar studies of the effect of PP fibre dosage on fire spalling were carried out. Li et al. **[23]** found that ultra-high-performance concrete with 3 kg/m^3 PP fibres by volume did not spall. Xiong and Liew **[37]** investigated UHSC with different PP fibre dosages in fire. The test results indicated that 0.1% PP fibres is effective to prevent spalling of the UHSC of strength over 150 MPa under high temperature up to 800 °C regardless of heating rate. However, previous studies **[25, 32-35, 37，50]** also indicated that the optimal fibre dosages resulted from such experimental parametric studies could vary depending on the concrete mix, specimen size/shape, heating regime, loading, etc. Further study is still needed to quantify their influences on the optimal PP fibre dosages.

2.5.6 The effects of steel fibres

UHSC is brittle and steel fibres have been used to improve its ambient temperature ductility **[12-14]**. The effect of steel fibre on fire spalling is still unclear; the published results give pretty diverse views **[24, 38-40]**. In this paper, UHSC9 (w/b = 0.15 and steel fibre dosage = 78.5 kg/m^3) was designed to explore this further. Moderate spalling was observed, as shown in **Fig. 9(d)**, indicating that the steel fibres adopted in this study were not as effective as PP fibres in terms of fire spalling mitigation. Similar conclusions were drawn by Bei et al. **[39, 40]**. However, it was interesting that the addition of steel fibres delayed the initial spalling time and the spalling was less explosive compared to the specimens without steel fibres. It is speculated that the steel fibres might have improved the tensile strength of the concrete matrix to some extent, which delays the occurrence of fire spalling but is not adequate to completely mitigate spalling.

3. Experiments on fibre-reinforced UHSC encased columns

Fire resistance behaviour of concrete encased columns is often considered to be sufficient because the steel is insulated by the concrete cover effectively. However, the explosive spalling of columns could reduce or completely remove the concrete cover, causing the significant weakness of the fire performance of encased columns due to the mechanical properties decreasing. Thus, the risk of spalling should be investigate as the UHSC using 0.15% PP fibre was applied in the encased columns under load.

Zhou et al. [60] experimentally studied the performance of concrete-encased steel tube columns in fire. The concrete encasement experienced explosive spalling subject to 60MPa uniaxial compressive stresses which was the same as the compressive strength of concrete. The authors believed that the spalling was caused by differential thermal stresses, which is agreed by Herzt [61].

The previous sections focus on the testing of UHSC on the material level. It is also necessary to extend the study to structural member level. Parameters like loading conditions and reinforcement, which are not considered during the material level testing, are considered in this section. Two fibre-reinforced UHSC (FRUHSC) encased columns with different slenderness were tested subject to ISO 834. These tests aim to study the spalling behaviour of FRUHSC encased columns at large scale and to validate the optimal PP fibres dosage proposed in Section 2.5.5.

3.1 Specimens and materials

Fig. 13 shows the preparation of the columns, which are 1400 mm and 2500 mm in length, respectively. An end plate (20 mm thick) is welded to each end of the specimen. The longitudinal reinforcement bars are of 12 mm diameter. The stirrups are of 8mm diameter, at 80 mm spacing along the column height. The details of the specimens are shown in Fig. 14 and Table 6. The reinforcements are designed according to the Eurocodes [62, 63]. The concrete mix is of 0.15 w/b, 39.25 kg/m^3 steel fibre dosage (0.5% by volume) and 1.365 kg/m^3 PP fibre dosage (0.15% by volume). The adoption of steel fibres in this study is not particularly to study their effectiveness in fire spalling mitigation. Since steel fibres are commonly used in UHSC for ambient temperature ductility, the motive is to assess the behaviour of UHSC columns with steel fibres in fire. The specimens were cast as shown in Fig. 13(c). After the concrete encasement, the specimens were watered on a regular basis for proper curing so as to prevent the shrinkage cracking of concrete. To protect the furnace against spalled debris, the specimens were covered with stainless steel meshes made of 1 mm diameter wires and 20 mm spacing during the spalling tests.

Table 6 lists the geometric and material properties of the specimens, where f_c is the 28-day cubic compressive strength of FRUHSC. f_{ss}, f_{sl} and f_{st} are the yield strengths of the steel section, longitudinal reinforcements and stirrups, respectively. E_{ss}, E_{sl} and E_{st} are their elastic moduli.

According to EC4 **[62]**, the calculated ambient-temperature ultimate load N_u of FRUHSC1 is 8865.3 kN and that of FRUHSC2 is 9163.2 kN. To reflect the fire limited state design load, load ratios (applied load P_0 during testing divided by the ambient temperature capacity N_u,) of 0.38 and 0.56 were adopted for FRUHSC1 and FRUHSC2, respectively. Therefore, the applied load P_0 during fire testing was 3368.8 kN and 5131.4 kN for FRUHSC1 and FRUHSC2, respectively.

3.2 Test setup and procedure

Both specimens were loaded monotonically by a 10,000 kN pressure testing machine under displacement control. The heated length of the 2500 mm long column is 2100 mm, and that of the 1400 mm long column is 1000 mm. Pin-ended connections were adopted at both ends of each column to allow end rotation, as shown in **Fig. 15**.

The compressive load was applied in a displacement-controlled manner. Preloading, up to 20% of the calculated ambient temperature ultimate load, was applied to eliminate any equipment deformation. Prior to heating, the specimens were loaded at a rate of 200 kN/min until the targeted test load was reached. The specimens were heated following the ISO 834 standard fire **[49]**. The applied axial load remained constant during the test. The test was terminated when the displacement rate at the end of the column reached 3×column length/1000 mm/min proposed by reference **[65]**.

3.3 Test results and discussions

Figs. 16 and 17 show the failures of the two FRUHSC columns. As expected, overall buckling was the dominant failure mode of both specimens. This agrees with previous finding **[55]** that concrete encased concrete-filled steel tube columns with slenderness ratio of 22 would likely experience global buckling failure under compression in fire. At failure, the concrete crushed suddenly with a loud sound at the concave side, as shown in **Figs. 16(b)** and **17(b)**. Visible transverse cracks were observed at the convex side of the columns as shown in **Figs. 16(d)** and **17(d)**. The failure mode is similar to that of the high strength concrete encased steel composite columns at ambient temperature **[8]**. It is attributed to the steel fibre, which improves the ductility of UHSC. None of the two columns experienced fire spalling, confirming that the proposed 1.365 kg/m^3 PP fibre dosage is also effective in mitigating the fire spalling of the tested large scale columns subject to the described testing conditions.

4. Conclusions

This paper presents an experimental investigation of the explosive spalling of UHSC and FRUHSC encased columns subject to ISO 834 standard fire. A total of fifteen fire spalling tests were conducted on 115-135 MPa UHSC, focusing on the effects of w/b, specimen size, porosity, PP fibres and steel fibres. Two large scale FRUHSC encased columns were also tested under simultaneous heating and loading. The following conclusions could be drawn based on the findings of this study:

(1) It is proposed that 1.365 kg/m^3 (0.15% by volume) is the optimal PP fibre dosage to prevent 115-135 MPa UHSC from explosive spalling, which is lower than the dosage recommended in EC2. Steel fibres could only reduce the intensity of the explosive fire spalling, but not prevent it.

(2) Given that the porosity of UHSC is generally low, the porosity of the 115-135 MPa UHSC does not have a significant influence on the fire spalling behaviour of UHSC. There is no distinct relationship between the inner concrete temperature and the occurrence of fire spalling. As the cylinder specimen with PP fibre dosages above 1.365 kg/m^3 scales up from Ø100 mm × 200 mm to Ø300 mm × 300 mm, the increase in specimen size did not influence the fire spalling or cracking behaviour.

(3) The large scale column specimens, which were cased with the FRUHSC proposed by this study, displayed no explosive spalling under axial load exposed to ISO834 fire. It confirmed the effectiveness of 1.365 kg/m^3 PP fibre in fire spalling mitigation at structural element level. The steel fibre dosage of 78.5 kg/m^3 can efficiently improve the ductility of the FRUHSC column specimens in fire.

(4) In terms of workability, 1.365 kg/m^3 PP fibres combined with 78.5 kg/m^3 steel fibres are suitable for the casting of the large scale columns.

Declaration of Competing Interest

None.

Acknowledgements

The research reported in this paper was supported by National Natural Science Foundation of China [Project number: 51878348]; National Key Research & Development Program of China [Project number: 2018YFC0705704]; International Centre for Integrated Protection Research of Engineering Structures (I-CIPRES) in Nanjing Tech University, China.

References

[1] Golafshani, E. M., & Behnood, A. (2019). Estimating the optimal mix design of silica fume concrete using biogeography-based programming. Cement and Concrete Composites, 96, 95-105.

[2] Siddique, R., & Chahal, N. (2011). Use of silicon and ferrosilicon industry by-products (silica fume) in cement paste and mortar. Resources, Conservation & Recycling, 55(8), 739-744.

[3] Siddique, R. (2011). Utilization of silica fume in concrete: Review of hardened properties. Resources, Conservation & Recycling, 55(11), 923-932.

[4] Behnood, A., & Golafshani, E. M. (2018). Predicting the compressive strength of silica fume concrete using hybrid artificial neural network with multi-objective grey wolves. Journal of Cleaner Production, 202, 54-64.

[5] Felekoğlu, B., & Sarıkahya, H. (2008). Effect of chemical structure of polycarboxylate-based superplasticizers on workability retention of self-compacting concrete. Construction and Building Materials, 22(9), 1972-1980.

[6] Šiler, P., Krátký, J., Kolářová, I., Havlica, J., & Brandštetr, J. (2013). Calorimetric determination of the effect of additives on cement hydration process. Chemical Papers, 67(2), 213-220.

[7] Khayat, K. H. (1999). Workability, testing, and performance of self-consolidating concrete. Materials Journal, 96(3), 346-353.

[8] Lai, B., Richard Liew, J. Y., & Wang, T. (2019). Buckling behaviour of high strength concrete encased steel composite columns. Journal of Constructional Steel Research, 154, 27-42.

[9] Kim, C., Park, H., Chung, K., & Choi, I. (2012). Eccentric axial load testing for concrete-encased steel columns using 800 MPa steel and 100 MPa concrete. Journal of Structural Engineering, 138(8), 1019-1031.

[10] Lai, B., Liew, J. Y. R., & Hoang, A. L. (2019). Behavior of high strength concrete encased steel

composite stub columns with C130 concrete and S690 steel. Engineering Structures, 200, 109743.

[11] Lai, B., Liew, J. Y. R., & Xiong, M. (2019). Experimental study on high strength concrete encased steel composite short columns. Construction and Building Materials, 228, 116640.

[12] Mousavi, S. M., Ranjbar, M. M., & Madandoust, R. (2019). Combined effects of steel fibers and water to cementitious materials ratio on the fracture behavior and brittleness of high strength concrete. Engineering Fracture Mechanics, 216, 106517.

[13] Kazemi, M. T., Fazileh, F., & Ebrahiminezhad, M. A. (2007). Cohesive crack model and fracture energy of steel-fiber-reinforced-concrete notched cylindrical specimens. Journal of Materials in Civil Engineering, 19(10), 884-890.

[14] Şahin, Y., & Köksal, F. (2011). The influences of matrix and steel fibre tensile strengths on the fracture energy of high-strength concrete. Construction and Building Materials, 25(4), 1801-1806.

[15] Noumowe, A. (2005). Mechanical properties and microstructure of high strength concrete containing polypropylene fibres exposed to temperatures up to 200 °C. Cement and Concrete Research, 35(11), 2192-2198.

[16] Janotka, I., & Nürnbergerová, T. (1999). Thermo-mechanical properties of penly reactor envelope at temperatures up to 200°C. Materials and Structures, 32(10), 719-726.

[17] Akca, A. H., & Özyurt Zihnioğlu, N. (2013). High performance concrete under elevated temperatures. Construction and Building Materials, 44, 317-328.

[18] Ding, Y., Azevedo, C., Aguiar, J. B., & Jalali, S. (2012;2011;). Study on residual behaviour and flexural toughness of fibre cocktail reinforced self compacting high performance concrete after exposure to high temperature. Construction and Building Materials, 26(1), 21-31.

[19] Aslani, F., Aslani, F., Samali, B., & Samali, B. (2014). High strength polypropylene fibre reinforcement concrete at high temperature. Fire Technology, 50(5), 1229-1247.

[20] Düğenci, O., Haktanir, T., & Altun, F. (2015). Experimental research for the effect of high temperature on the mechanical properties of steel fiber-reinforced concrete. Construction and Building Materials, 75, 82-88.

[21] Ding, Y., Zhang, C., Cao, M., Zhang, Y., & Azevedo, C. (2016). Influence of different fibers on the change of pore pressure of self-consolidating concrete exposed to fire. Construction and Building Materials, 113, 456-469.

[22] Kalifa, P., Menneteau, F., & Quenard, D. (2000). Spalling and pore pressure in HPC at high

temperatures. Cement and Concrete Research, 30(12), 1915-1927.

[23] Li, Y., Pimienta, P., Pinoteau, N., & Tan, K. H. (2019). Effect of aggregate size and inclusion of polypropylene and steel fibers on explosive spalling and pore pressure in ultra-high-performance concrete (UHPC) at elevated temperature. Cement and Concrete Composites, 99, 62-71.

[24] Kodur, V. K. R., & Phan, L. (2007). Critical factors governing the fire performance of high strength concrete systems. Fire Safety Journal, 42(6), 482-488.

[25] Heo, Y., Sanjayan, J. G., Han, C., & Han, M. (2012). Relationship between inter-aggregate spacing and the optimum fiber length for spalling protection of concrete in fire. Cement and Concrete Research, 42(3), 549-557.

[26] Cülfik, M. S., & Özturan, T. (2010). Mechanical properties of normal and high strength concretes subjected to high temperatures and using image analysis to detect bond deteriorations. Construction and Building Materials, 24(8), 1486-1493.

[27] Giaccio, G. M. (2005). Mechanical behaviour of thermally damaged high-strength steel fibre reinforced concrete. Materials and Structures, 38(277), 335-342.

[28] Toropovs, N., Lo Monte, F., Wyrzykowski, M., Weber, B., Sahmenko, G., Vontobel, P., Lura, P. (2015). Real-time measurements of temperature, pressure and moisture profiles in high-performance concrete exposed to high temperatures during neutron radiography imaging. Cement and Concrete Research, 68, 166-173.

[29] Liu, X., Ye, G., De Schutter, G., Yuan, Y., & Taerwe, L. (2008). On the mechanism of polypropylene fibres in preventing fire spalling in self-compacting and high-performance cement paste. Cement and Concrete Research, 38(4), 487-499.

[30] Liu, J., Tan, K. H., & Yao, Y. (2018). A new perspective on nature of fire-induced spalling in concrete. Construction and Building Materials, 184, 581-590.

[31] Zhang, D., Dasari, A., & Tan, K. H. (2018). On the mechanism of prevention of explosive spalling in ultra-high performance concrete with polymer fibers. Cement and Concrete Research, 113, 169-177.

[32] Suhaendi, S. L., & Horiguchi, T. (2006). Effect of short fibers on residual permeability and mechanical properties of hybrid fibre reinforced high strength concrete after heat exposition. Cement and Concrete Research, 36(9), 1672-1678.

[33] Garboczi, E., Snyder, K., Douglas, J., & Thorpe, M. (1995). Geometrical percolation threshold of overlapping ellipsoids. Physical Review. E, Statistical Physics, Plasmas, Fluids, and Related

Interdisciplinary Topics, 52(1), 819-828.

[34] Heo, Y., Sanjayan, J. G., Han, C., & Han, M. (2010). Synergistic effect of combined fibers for spalling protection of concrete in fire. Cement and Concrete Research, 40(10), 1547-1554.

[35] Heo, Y., Heo, Y., Sanjayan, J. G., Sanjayan, J. G., Han, C., Han, C., . . . Han, M. (2011). Critical parameters of nylon and other fibres for spalling protection of high strength concrete in fire. Materials and Structures, 44(3), 599-610.

[36] Narayanan, R. S., & Beeby, A. W. (2005). EN 1992-1-2. Eurocode 2: Design of Concrete Structures: General Rules. Thomas Telford.

[37] Xiong, M. X., & Liew, J. R. (2015). Spalling behavior and residual resistance of fibre reinforced Ultra-High performance concrete after exposure to high temperatures. Materiales de Construcción, 65(320), 071.

[38] Kodur, V. K. R., Cheng, F., Wang, T., & Sultan, M. A. (2003). Effect of strength and fiber reinforcement on fire resistance of high-strength concrete columns. Journal of Structural Engineering, 129(2), 253-259.

[39] Bei, S., & Zhixiang, L. (2016). Investigation on spalling resistance of ultra-high-strength concrete under rapid heating and rapid cooling. Case Studies in Construction Materials, 4(C), 146-153.

[40] Sideris, K., Manita, P., Papageorgiou, A., & Chaniotakis, E., (2006). Mechanical characteristic of high performance fiber reinforced concretes at elevated temperatures, ACI Special Publication, 212(60),973–988.

[41] Abdallah, S., Fan, M., & Cashell, K. A. (2017). Bond-slip behaviour of steel fibres in concrete after exposure to elevated temperatures. Construction and Building Materials, 140, 542-551.

[42] Bangi, M. R., & Horiguchi, T. (2012). Effect of fibre type and geometry on maximum pore pressures in fibre-reinforced high strength concrete at elevated temperatures. Cement and Concrete Research, 42(2), 459-466.

[43] Haddadou, N., Chaid, R., & Ghernouti, Y. (2015). Experimental study on steel fibre reinforced self-compacting concrete incorporating high volume of marble powder. European Journal of Environmental and Civil Engineering, 19(1), 48-64.

[44] Schutter, G., (2005). Guidelines for testing fresh self-compacting concrete.

[45] Concrete, S. C. (2005). The European Guidelines for Self-Compacting Concrete. BIBM, et al, 22.

[46] Missemer, L., Ouedraogo, E., Malecot, Y., Clergue, C., & Rogat, D. (2019). Fire spalling of

ultra-high performance concrete: From a global analysis to microstructure investigations. Cement and Concrete Research, 115, 207-219.

[47] Felicetti, R., Gambarova, P. G., Sora, M. N., & Khoury, G. A. (2000, September). Mechanical behaviour of HPC and UHPC in direct tension at high temperature and after cooling. In Fifth RILEM symposium on fibre-reinforced concretes, N (pp. 749-758).

[48] Durrani, A.J., Castillo, C., (1990). Effect of transient high temperature on high strength concrete, ACI Materials Journal, 35(1),47–53.

[49] ISO 834-1:1999. (2020, January 15). Retrieved from https://www.iso.org/standard/2576.html

[50] Boström, L., Wickström, U., & Adl‐Zarrabi, B. (2007). Effect of specimen size and loading conditions on spalling of concrete. Fire and Materials, 31(3), 173-186.

[51] Ali, F. A., O'Connor, D., & Abu-Tair, A. (2001). Explosive spalling of high-strength concrete columns in fire. Magazine of Concrete Research, 53(3), 197-204.

[52] Lee, J. H., Sohn, Y. S., & Lee, S. H. (2012). Fire resistance of hybrid fibre-reinforced, ultra-high-strength concrete columns with compressive strength from 120 to 200 MPa. Magazine of concrete research, 64(6), 539-550.

[53] Aldea, C. M., Franssen, J. M. & Dotreppe, J. C. (1997). Fire Tests on Normal and High Strength Reinforced Concrete Columns, NIST special publication , 919,109-117.

[54] Lennon, T. & Clayton, N. (1998) Programme to Investigate the Performance of High Strength Concrete in Fire, With Particular Reference to Explosive Spalling. BRE Ltd Report. FG 2837, (Note N23/98).

[55] Kalifa, P., Chéné, G., & Gallé, C. (2001). High-temperature behaviour of HPC with polypropylene fibres: From spalling to microstructure. Cement and Concrete Research, 31(10), 1487-1499.

[56] Zegardło, B., Szeląg, M., & Ogrodnik, P. (2018). Concrete resistant to spalling made with recycled aggregate from sanitary ceramic wastes – the effect of moisture and porosity on destructive processes occurring in fire conditions. Construction and Building Materials, 173, 58-68.

[57] Rossino, C., Monte, F. L., Cangiano, S., Felicetti, R., & Gambarova, P. G. (2013). Concrete spalling sensitivity versus microstructure: Preliminary results on the effect of polypropylene fibers. In MATEC Web of Conferences (Vol. 6, p. 02002). EDP Sciences.

[58] Mindeguia, J., Carré, H., Pimienta, P., & La Borderie, C. (2015). Experimental discussion on the mechanisms behind the fire spalling of concrete. Fire and Materials, 39(7), 619-635.

[59] Poon, C., Azhar, S., Anson, M., & Wong, Y. (2001). Comparison of the strength and durability performance of normal- and high-strength pozzolanic concretes at elevated temperatures. Cement and Concrete Research, 31(9), 1291-1300.

[60] Zhou, K., & Han, L. (2018). Experimental performance of concrete-encased CFST columns subjected to full-range fire including heating and cooling. Engineering Structures, 165, 331-348.

[61] Hertz, K. D. (2003). Limits of spalling of fire-exposed concrete. Fire Safety Journal, 38(2), 103-116.

[62] Johnson, R. P., & Anderson, D. (2004). Designers' Guide to EN 1994-1-1: Eurocode 4: Design of Composite Steel and Concrete Structures. General Rules and Rules for Buildings. Thomas Telford.

[63] Johnson, R. P., & Anderson, D. (2005). Designers' Guide to EN 1994-1-2: Eurocode 4: Design of Composite Steel and Concrete Structures. General Rules-Structural Fire Design. Thomas Telford.

[64] Liang, X., Wu, C., Su, Y., Chen, Z., & Li, Z. (2018). Development of ultra-high performance concrete with high fire resistance. Construction and Building Materials, 179, 400-412.

[65] GB/T 9978.1-2008, Fire-resistance tests-Elements of building construction. (in Chinese)

Fig. 1 Practical case and typical cross section of concrete encased columns

(a) PP fibre

(b) Steel fibre

Fig. 2 PP and steel fibres

(a) Slump-flow test

(b) J-ring test

(c) L-box test

Fig. 3 The measurements of the fresh properties of concrete

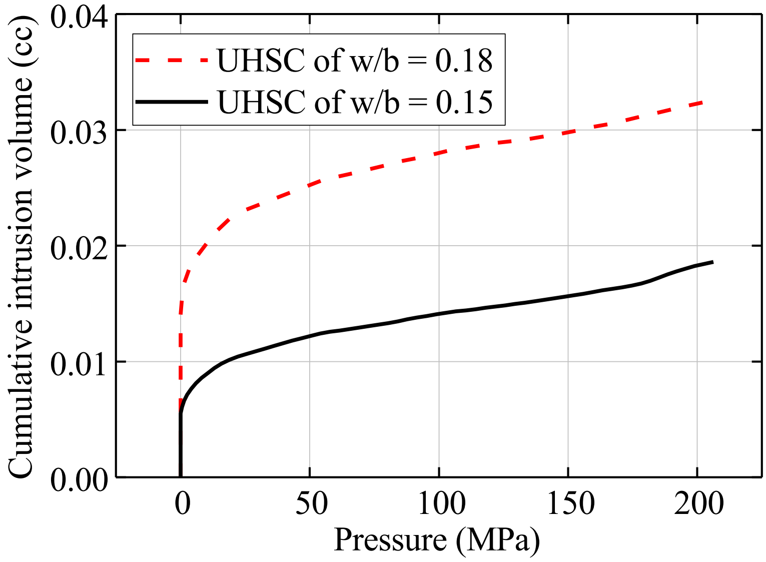

Fig. 4 Cumulative intrusion volume of plain UHSC with different w/b

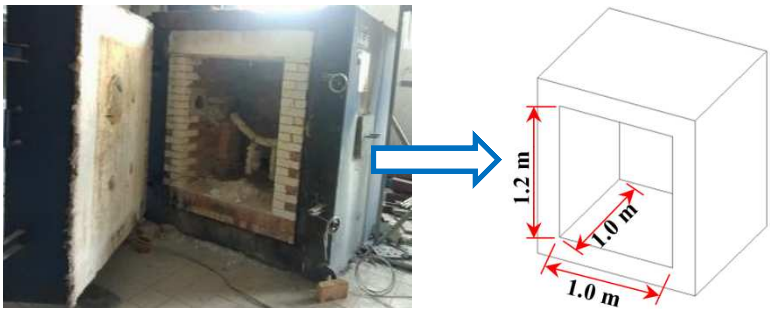

Fig. 5 Gas furnace

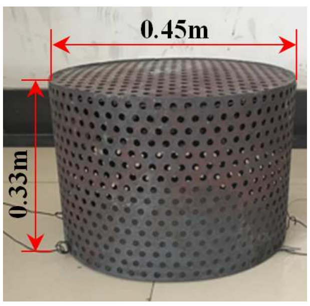

Fig. 6 Protective steel cage

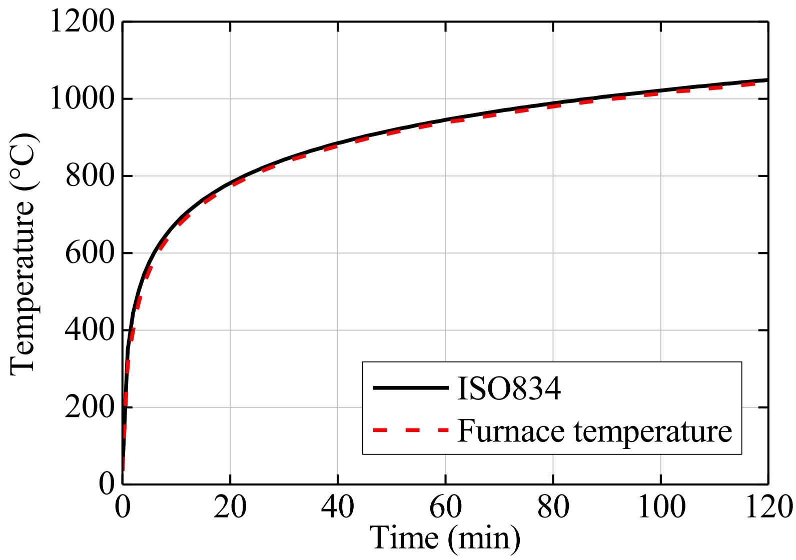

Fig. 7 Temperature-time curve of ISO 834 and furnace without specimen


(a) UHSC1


(b) UHSC2


(c) UHSC3

(d) UHSC4


(e) UHSC5

Fig. 8 Failure modes of UHSC specimens with w/b of 0.18 (Ø300×300 mm)

(a) UHSC6

(b) UHSC7

(c) UHSC8


(d) UHSC9

(e) UHSC10

(f) UHSC11

(g) UHSC12

Fig. 9 Failure modes of UHSC specimens with w/b of 0.15 (Ø300×300 mm)

(a) UHSC13 (b) UHSC14 (c) UHSC15

Fig. 10 Failure modes of UHSC specimens with w/b of 0.15 (Ø100×200 mm)

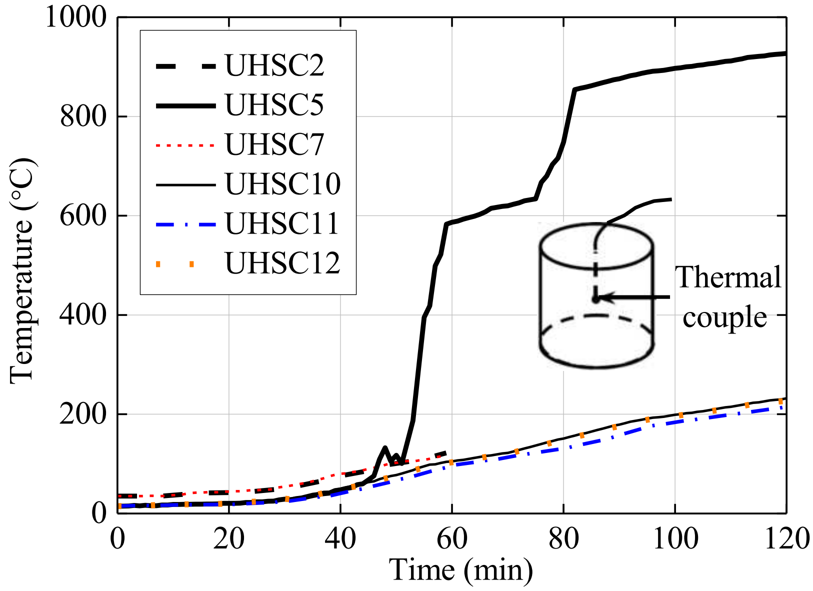

Fig. 11 Inner concrete temperature as a function of heating time

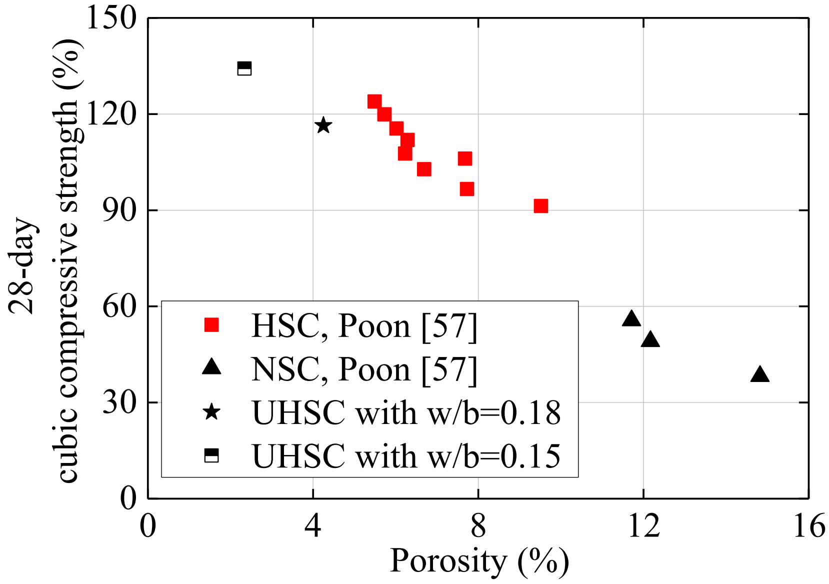

Fig. 12 28-day cubic compressive strength against porosity

(a) Reinforcement cage installation (b) Formwork erection (c) Concrete casting (d) Specimen completion

Fig. 13 Preparation of FRUHSC encased column specimen

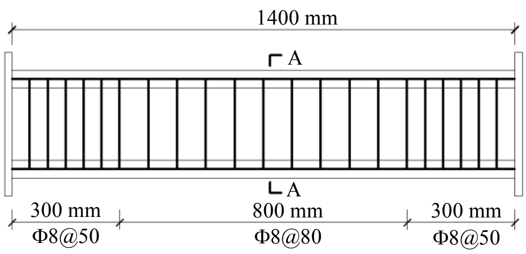

(a) The details of the 1400 mm long specimen

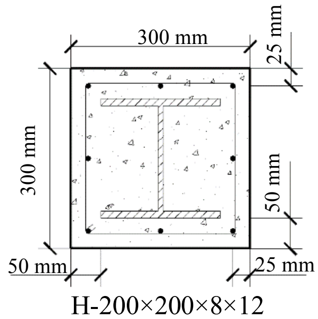

(b) Cross-section A-A

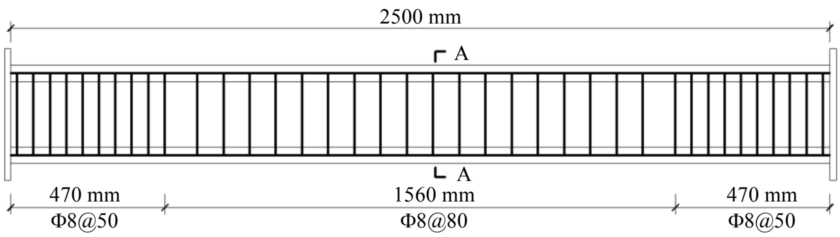

(c) The details of the 2500 mm long specimen

Fig. 14 The schematic of FRUHSC encased columns

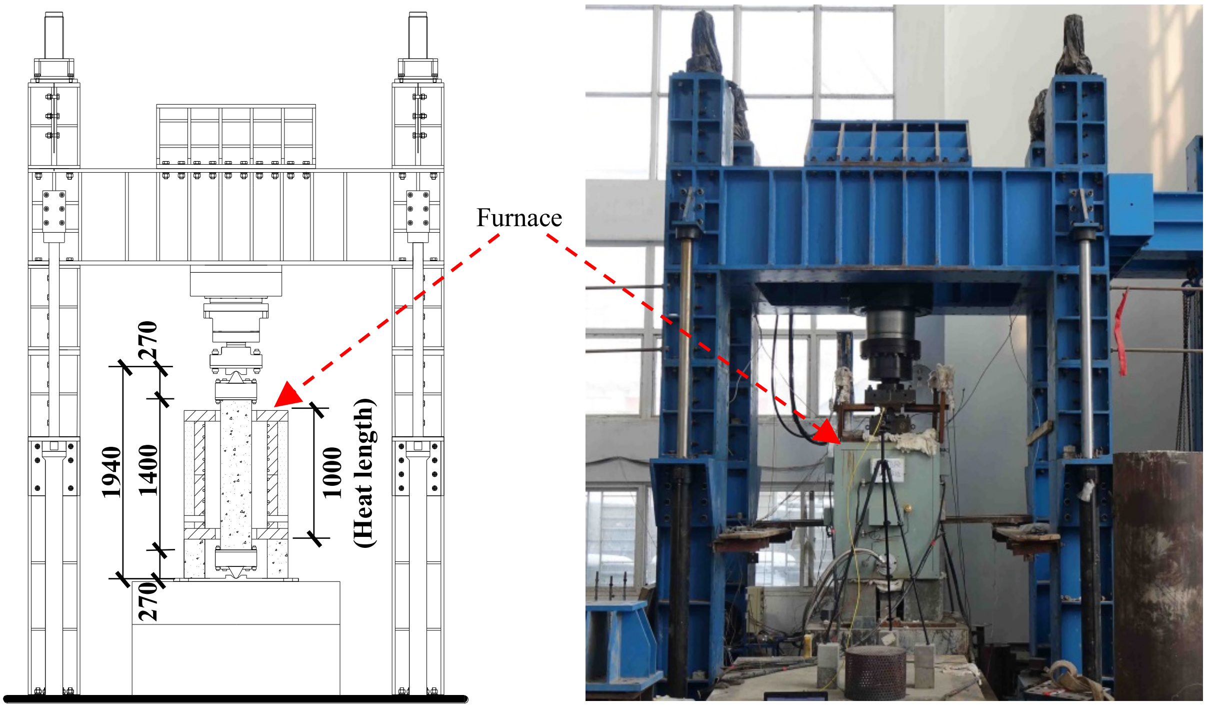

(a) Test setup of FRUHSC1

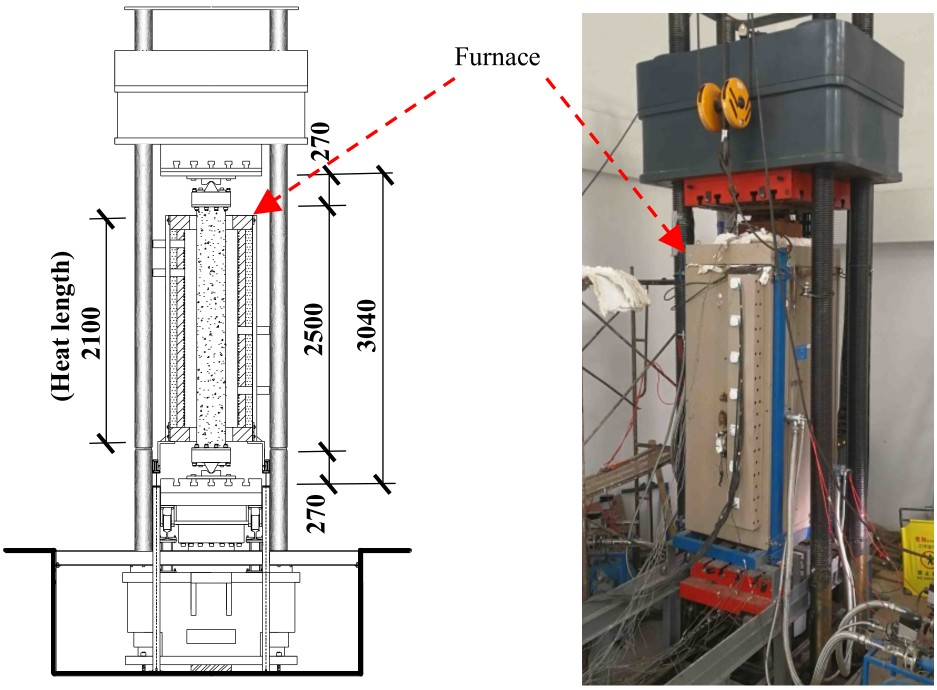

(b) Test setup of FRUHSC2

Fig. 15 Test setup of FRUHSC encased columns

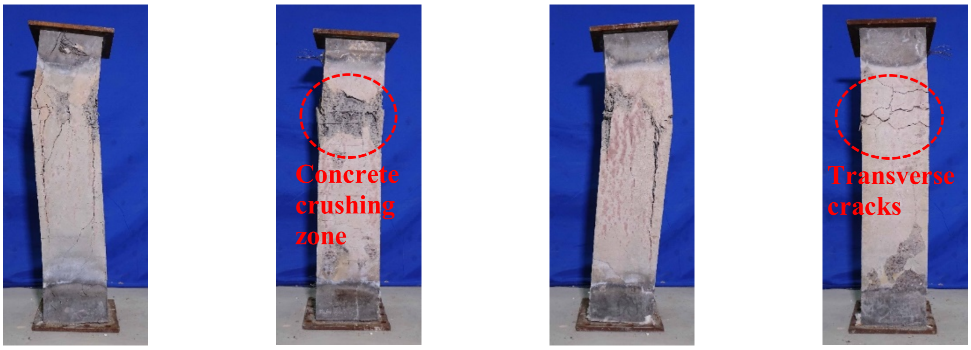

(a) Side 1 (b) Side 2 (c) Side 3 (d) Side 4

Fig. 16 The failure of FRUHSC encased column, 1400 mm in length

(a) Side 1 (b) Side 2 (c) Side 3 (d) Side 4

Fig. 17 The failure of FRUHSC encased column, 2500 mm in length

Table 1 Fibre properties

Type	Density (kg/m^3)	Melting point (℃)	Diameter (μm)	Length (mm)	Cross-sectional shape
PP fibre	910	170	18	16	Circular
Steel fibre	7850	1535	230	14	Circular

Table 2 UHSC mix designs and 28-day compressive strengths

Series	w/b	Cement (kg/m^3)	Silica fume (kg/m^3)	Water (kg/m^3)	Sand (kg/m^3)	Coarse aggregate (kg/m^3)	Superplasticizer (kg/m^3)	28-day cube strength* (MPa)
I	0.18	810	90	162	588	882	18	117(3.42)
II	0.15	821	91	137	593	890	18	134(1.71)

* Standard deviation is presented in the parenthesis after the average value from three specimens

Table 3 Fresh property tests on UHSC

Sample No.	w/b	Steel fibre (kg/m^3)	PP fibre (kg/m^3)	S (mm)	T_{500} (s)	PA (mm)	H_2/H_1	Observation
1	0.18	0	0	750	5	22	0.92	Slight segregation
2		39.25	0	720	5	25	0.90	Slight segregation
3		78.5	0	680	7	31	0.85	Slight segregation
4		117.75	0	670	9	32	0.74	Slight segregation
5	0.15	0	0	640	8	20	0.87	No segregation
6		39.25	0	620	9	25	0.85	No segregation
7		78.5	0	590	12	29	0.64	No segregation
8		117.75	0	520	15	38	0.43	No segregation
9		0	0.91	600	8	24	0.82	No segregation
10		0	1.365	560	10	30	0.58	No segregation
11		0	2	510	13	37	0.25	No segregation
12		39.25	1.365	520	14	40	0.2	No segregation
13		78.5	2	450	/	70	0	Significantly reduced flowability

Table 4 A summary of the UHSC specimens for the fire spalling tests

Specimen ID	w/b	Dimension (mm)	PP fibre		Steel fibre	
			(kg/m^3) by mass	(%) by volume	(kg/m^3) by mass	(%) by volume
UHSC1	0.18	Ø300×300	0.91	0.1	0	0
UHSC2			2	0.22	0	0
UHSC3			1.365	0.15	11.775	0.15
UHSC4			1.365	0.15	23.55	0.3
UHSC5			0	0	0	0
UHSC6	0.15	Ø300×300	2.73	0.3	11.775	0.15
UHSC7			4.55	0.5	11.775	0.15
UHSC8			2	0.22	0	0
UHSC9			0	0	78.5	1
UHSC10			0.91	0.1	0	0
UHSC11			1.183	0.13	0	0
UHSC12			1.365	0.15	0	0
UHSC13	0.15	Ø100×200	0.91	0.1	0	0
UHSC14			1.183	0.13	0	0
UHSC15			1.365	0.15	0	0

Table 5 Spalling test results and compressive strength

Specimen ID	PP fibre		Steel fibre		Compressive strength (MPa)	Spalling magnitude	Spalling depth d_s (mm)	Spalling area ratio δ_s (%)
	(kg/m^3) by mass	(%) by volume	(kg/m^3) by mass	(%) by volume				
UHSC1	0.91	0.1	0	0	116.4	Slight	0	0
UHSC2	2	0.22	0	0	118.0	No	0	0
UHSC3	1.365	0.15	11.775	0.15	122.3	No	0	0
UHSC4	1.365	0.15	23.55	0.3	127.6	No	0	0
UHSC5	0	0	0	0	117.8	Collapse	N.A.*	N.A.
UHSC6	2.73	0.3	11.775	0.15	142.6	No	0	0
UHSC7	4.55	0.5	11.775	0.15	136.5	No	0	0
UHSC8	2	0.22	0	0	134.2	No	0	0
UHSC9	0	0	78.5	1	134.5	Intensive	47	63
UHSC10	0.91	0.1	0	0	122.5	Intensive	38	28
UHSC11	1.183	0.13	0	0	133.4	Great	24	9
UHSC12	1.365	0.15	0	0	130.1	No	0	0
UHSC13	0.91	0.1	0	0	122.5	Moderate	13	18
UHSC14	1.183	0.13	0	0	133.4	Moderate	6	14
UHSC15	1.365	0.15	0	0	130.1	No	0	0

* N.A. notes that measurements could not be performed due to the severe condition of the specimens

Table 6 The geometric and material properties of the columns

Specimen		FRUHSC1	FRUHSC2
Geometric properties	Section size (mm×mm)	300×300	300×300
	Steel profile (height×width×web thickness×flange thickness in mm)	200×200×8×12	200×200×8×12
	Length L (mm)	1400	2500
	Heated length L_e (mm)	1000	2100
	Slenderness ratio $\lambda=2\sqrt{3}L/H$	16.2	28.9
	Link space (mm)	80	80
	Steel area ratio A_s/A	7.9%	7.9%
Material properties	f_c (MPa)	126.8	129.3
	f_{ss} (MPa)	379.6	379.6
	f_{sl} (MPa)	523.9	523.9
	f_{st} (MPa)	489.8	489.8
	E_{ss} (GPa)	204.4	204.4
	E_{sl} (GPa)	192.3	192.3
	E_{st} (GPa)	244.0	244.0

Appendix A.

Table A.1. Summary of the spalling test results of UHSC in previous studies

Source	Dimension (mm)	28-day compressive strength (MPa)	Aggregate	w/b	PP fibre (kg/m^3)	Steel fibre (kg/m^3)	Spalling magnitude	Spalling depth (mm)	Spalling area (%)	Weight loss (%)	Failure mode
Li et al. [23]	50×50×50	149.6	River sand (No coarse aggregate)	0.22	0	0	Intensive	<5	10-150	/*	
Li et al. [23]	50×50×50	159.7	River sand (No coarse aggregate)	0.22	3	0	No	0	0	/	
Li et al. [23]	50×50×50	172.1	River sand (No coarse aggregate)	0.22	0	196.3	Intensive	<5	10-150	/	
Li et al. [23]	50×50×50	154.8	River sand (No coarse aggregate)	0.22	3	196.3	No	0	0	/	
Xiong and Liew [37]	Ø100×200	155.8	Bauxite (No coarse aggregate)	0.076[A]	4.55	39.25	No	/	/	/	/
Xiong and Liew [37]	Ø100×200	163	Bauxite (No coarse aggregate)	0.076	0	0	Collapse	/	/	/	/
Xiong and Liew [37]	Ø100×200	172	Bauxite (No coarse aggregate)	0.076	0.91	0	No	/	/	/	/
Xiong and Liew [37]	Ø100×200	151	Bauxite (No coarse aggregate)	0.076	2.275	0	No	/	/	/	/
Xiong and Liew [37]	Ø100×200	147	Bauxite (No coarse aggregate)	0.076	4.55	0	No	/	/	/	/
Lee et al. [52]	300×300×450	129.1	Granite	0.11	3.458	39.25	Slight	4.1	1.9	10	/
Lee et al. [52]	300×300×450	135.2	Granite	0.11	3.458	39.25	Moderate	6.1	19.4	9.5	/
Lee et al. [52]	300×300×450	129.1	Granite	0.11	4.004	39.25	Intensive	30.9	54.7	9.4	/
Lee et al. [52]	300×300×450	144.4	Granite	0.11	4.55	39.25	Moderate	10	18.6	8.3	/

Table A.1. (Continued)

Source	Dimension (mm)	28-day compressive strength (MPa)	Aggregate	w/b	PP fibre (kg/m3)	Steel fibre (kg/m3)	Spalling magnitude	Spalling depth (mm)	Spalling area (%)	Weight loss (%)	Failure mode
Lee et al. [52]	300×300×450	121.2	Granite	0.11	4.55	39.25	No	0	0	8.8	/
Lee et al. [52]	300×300×450	124	Granite	0.11	5.46	39.25	Slight	2	2.4	9.2	/
Lee et al. [52]	300×300×450	188.3	EAF slag	0.11	3.458	39.25	Intensive	75.6	92	25.6	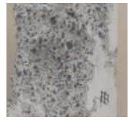
Lee et al. [52]	300×300×450	148.6	Granite	0.11	3.458	78.5	Slight	4	2.8	5.5	/
Lee et al. [52]	300×300×450	177.2	EAF slag	0.11	4.55	39.25	Intensive	39.7	54.6	16.8	/
Lee et al. [52]	300×300×450	167.6	EAF slag	0.11	4.55	39.25	Intensive	22.3	58.6	16	/
Lee et al. [52]	300×300×450	186.5	Granite	0.125	0	0	Collapse	N.A.**	N.A.	100	/
Lee et al. [52]	300×300×450	175	Granite	0.125	3.64	0	Collapse	N.A.	N.A.	N.A.	/
Lee et al. [52]	300×300×450	167.8	Granite	0.125	5.46	0	Collapse	N.A.	N.A.	N.A.	/
Lee et al. [52]	300×300×450	193.1	Granite	0.125	0	39.25	Collapse	N.A.	N.A.	77.9	
Liang et al. [64]	50×50×50	112.4	Quartz sand (No coarse aggregate)	0.16	0	0	Collapse	/	/	N.A.	
Liang et al. [64]	50×50×50	187.5	Quartz sand (No coarse aggregate)	0.16	0	157	Collapse	/	/	N.A.	
Liang et al. [64]	50×50×50	125.5	Quartz sand (No coarse aggregate)	0.16	18.2	0	Moderate	/	/	9	
Liang et al. [64]	50×50×50	162.1	Quartz sand (No coarse aggregate)	0.16	18.2	78.5	Slight	/	/	8	

Table A.1. (Continued)

Source	Dimension (mm)	28-day compressive strength (MPa)	Aggregate	w/b	PP fibre (kg/m3)	Steel fibre (kg/m3)	Spalling magnitude	Spalling depth (mm)	Spalling area (%)	Weight loss (%)	Failure mode
Liang et al. [64]	50×50×50	90	Steel slag (No coarse aggregate)	0.16	0	0	Collapse	/	/	N.A.	
Liang et al. [64]	50×50×50	162.8	Steel slag (No coarse aggregate)	0.16	18.2	78.5	Slight	/	/	7.5	

[A] 0.076 is the value of water/commercial concrete product
* / notes that no test or photograph is shown in the paper
** N.A. notes that measurements could not be performed due to the severe condition of the specimens